Subtask 3.1D

LES Analysis for Controlling Fuel Distribution in Diesel PCCI Combustion

Kazuie Nishiwaki
Ritsumeikan University
and
Takafumi Kojima
Takamatsu National College of Technology

Motivation and Purpose of the Study

- Switching the combustion mode between Diesel and PCCI has a potential to improve the emissions performance.

  - Diesel combustion mode at high load / the exhaust gas temperature is high enough to keep a catalytic converter active.
  - PCCI combustion mode at low load / the exhaust gas temperature is too low for a catalytic converter to be active. Low emissions and high efficiency of the PCCI, the output of which is restricted to a partial load, has an advantage in such a condition.

- The purpose of the study to develop an efficient LES computer model and to systematically analyze the mixture formation in the PCCI combustion mode, varying the injection pressure and timing over a wide range from the view point of NO emission and pressure rise rate.

Outline of the Model

- CFD model
  - Transport equations for mass, momentum, enthalpy and species mass fractions in spatially filtered forms (LES)
  - Sub-grid kinematic viscosity: Smagorinsky model
  - Initial velocity field: Correlation Generating method

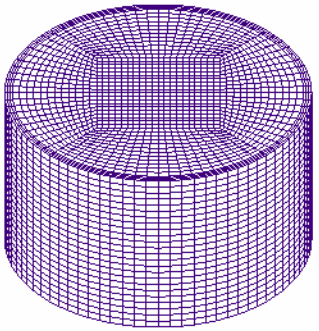

- Spray model to reduce computer load
  - Gas-jet model (Ikegami's model)

- Reaction kinetics to reduce computer load
  - Schreiber model
    – five step global reactions
  - Extended Zel'dovich model for thermal NO reaction

Gas Jet Model

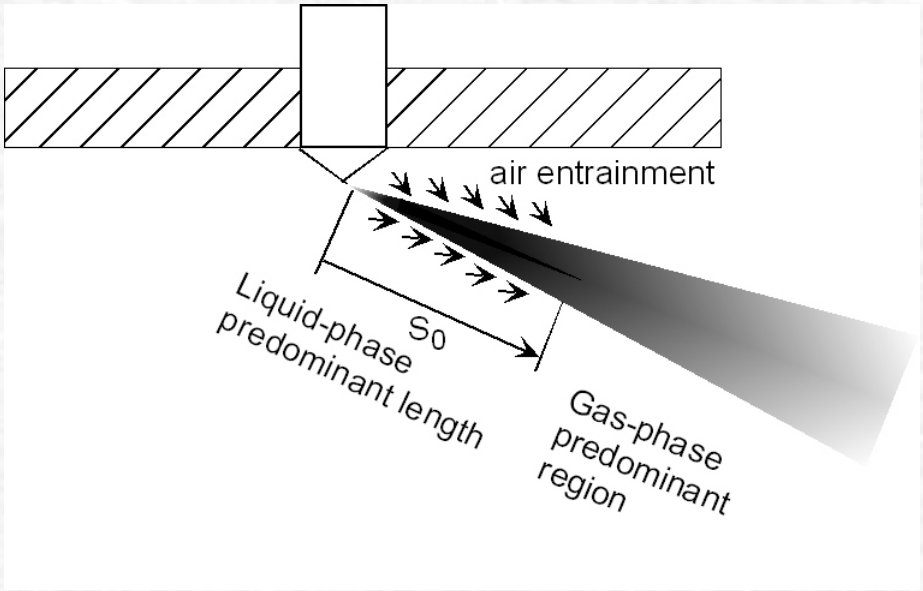

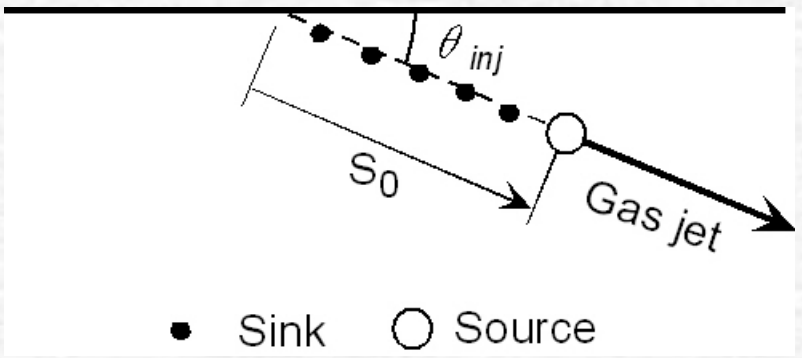

- The gas jet model
  - The sinks are models for air entrainment. The mass of air entrained is estimated by Wakuri's model
  - The source ejects the mixture of gasified fuel and air with the sum of momentum of the fuel injected and the air entrained through the sinks

Computational Conditions / 1 of 2

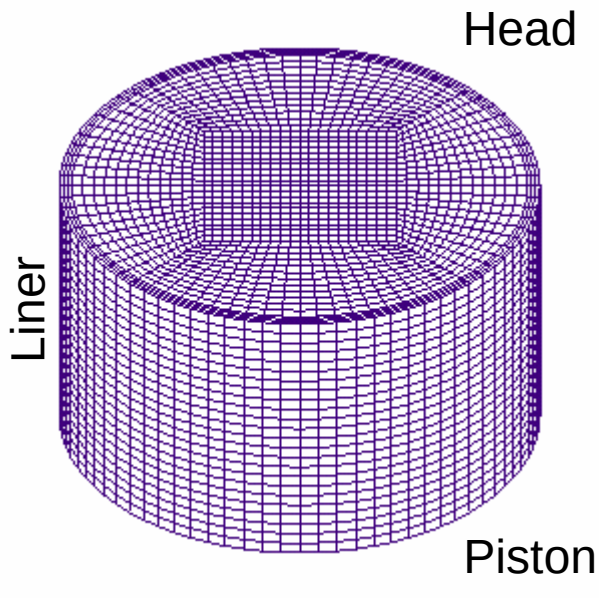

Total number of cells : 38,400
(Cell volume)$^{1/3}$ 3.0 - 1.5 mm
(bdc) (tdc)
Measured integral length scale in literature: 4-5mm - 2.5mm
(bdc) (tdc)

Engine conditions

Bore×Stroke	**: 82.6×114.3 mm**
Compression ratio	**: 12.0**
Engine speed	**: 1800 rpm**
Equivalence ratio	**: 0.38 (average)**
Swirl ratio	**: 0.5**
Intake valve closing	**: 146 deg . btdc**
EGR ratio	**: 7 %**
Wall temperature	**: 400 K, uniform**
Initial temperature	**: 323 K**
Initial pressure	**: 0.1 MPa**
Initial turbulence kinetic energy	**: 0.74 C_m^2 (C_m: mean piston speed)**
Fuel	**: n-Heptane**

Computational Conditions / 2 of 2

- **Injection conditions**

  Nozzle hole diameter d_n : 0.1, 0.2 mm
  Injection angle θ_{inj} : 30 deg.
  Liquid-phase predominant length S_0 : 20 mm
  Injection pressure p_{inj} : 40, 80, 120 MPa
  Injection time : 10, 20, 30, 40, 50, 60 btdc

- **2×3×6 different combinations of injection conditions**

- **Computing time : 15 to 20 hours each combination**

Spray Tip Penetration

p_{inj} MPa	d_n mm
40	0.1
80	0.1
40	0.2

Wakuri's model : $$x = \left(\frac{2c(p_{inj} - p_a)}{\rho_a} \right)^{0.25} \left(\frac{t\, d_n}{\tan\theta} \right)^{0.5}$$

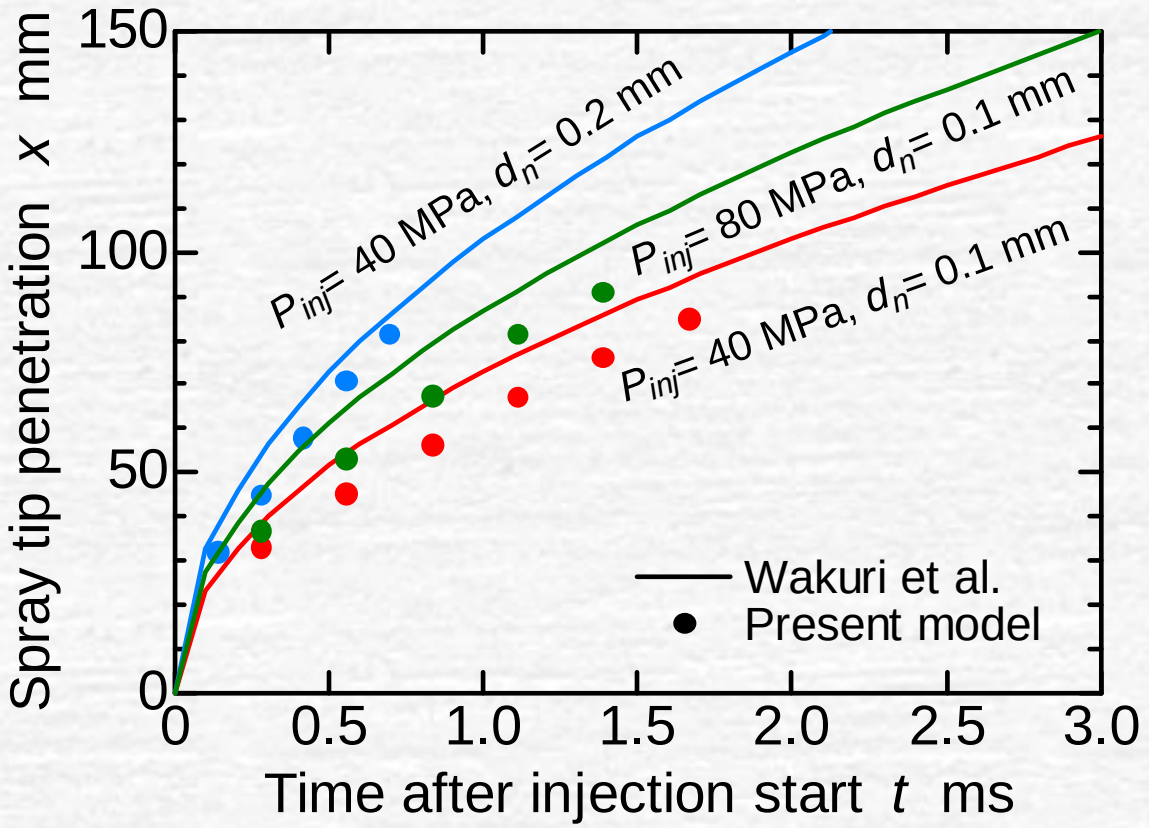

Mixture Formation – Gas Jet Model

No-combustion case/ p_{inj} = 40 MPa, d_n = 0.1 mm × 4 holes, I. T. = 60 deg. BTDC

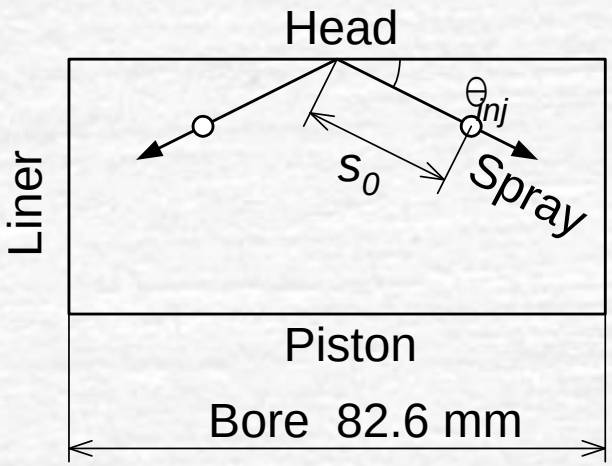

55 deg. BTDC

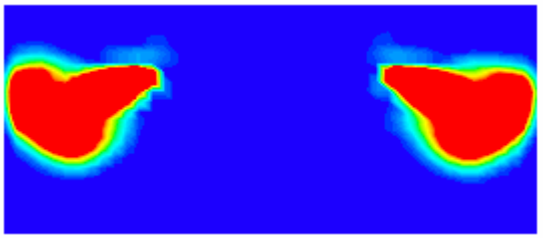

50 deg. BTDC

40 deg. BTDC

30 deg. BTDC

20 deg. BTDC

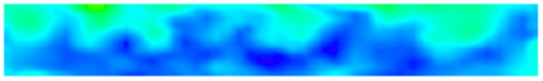

10 deg. BTDC

TDC

10 deg. ATDC

Local Heat Release Rate

p_{inj} = 120 MPa, d_n = 0.2 mm × 4 holes

ROHR 3000 kJ/(m3deg.) and over

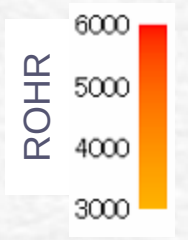

Peak ROHR

Injection timing = -10 deg.

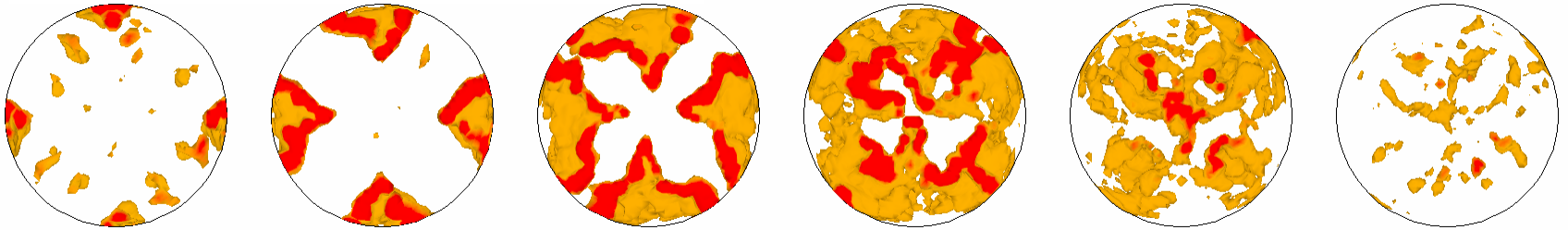

2 deg. 3 deg. 4 deg. 5 deg. 6 deg. 7 deg.

Injection timing = -30 deg.

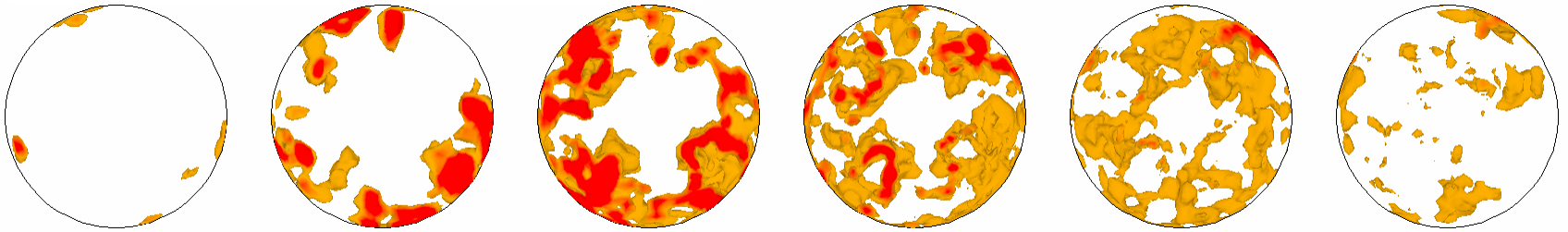

-4 deg. -3 deg. -2 deg. -1 deg. 0 deg. 1 deg.

Injection timing = -50 deg.

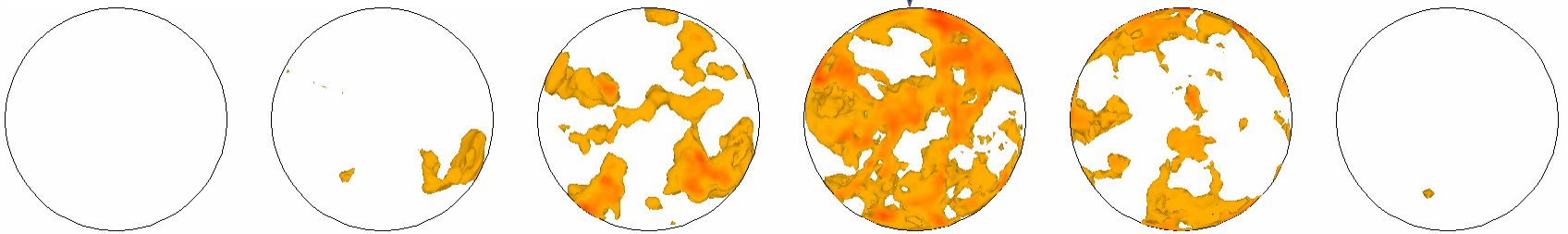

-3 deg. -2 deg. -1 deg. 0 deg. 1 deg. 2 deg.

Overall Heat Release Rates and PDF of Equivalence ratios

p_{inj} = 120 MPa, d_n = 0.2 mm × 4 holes

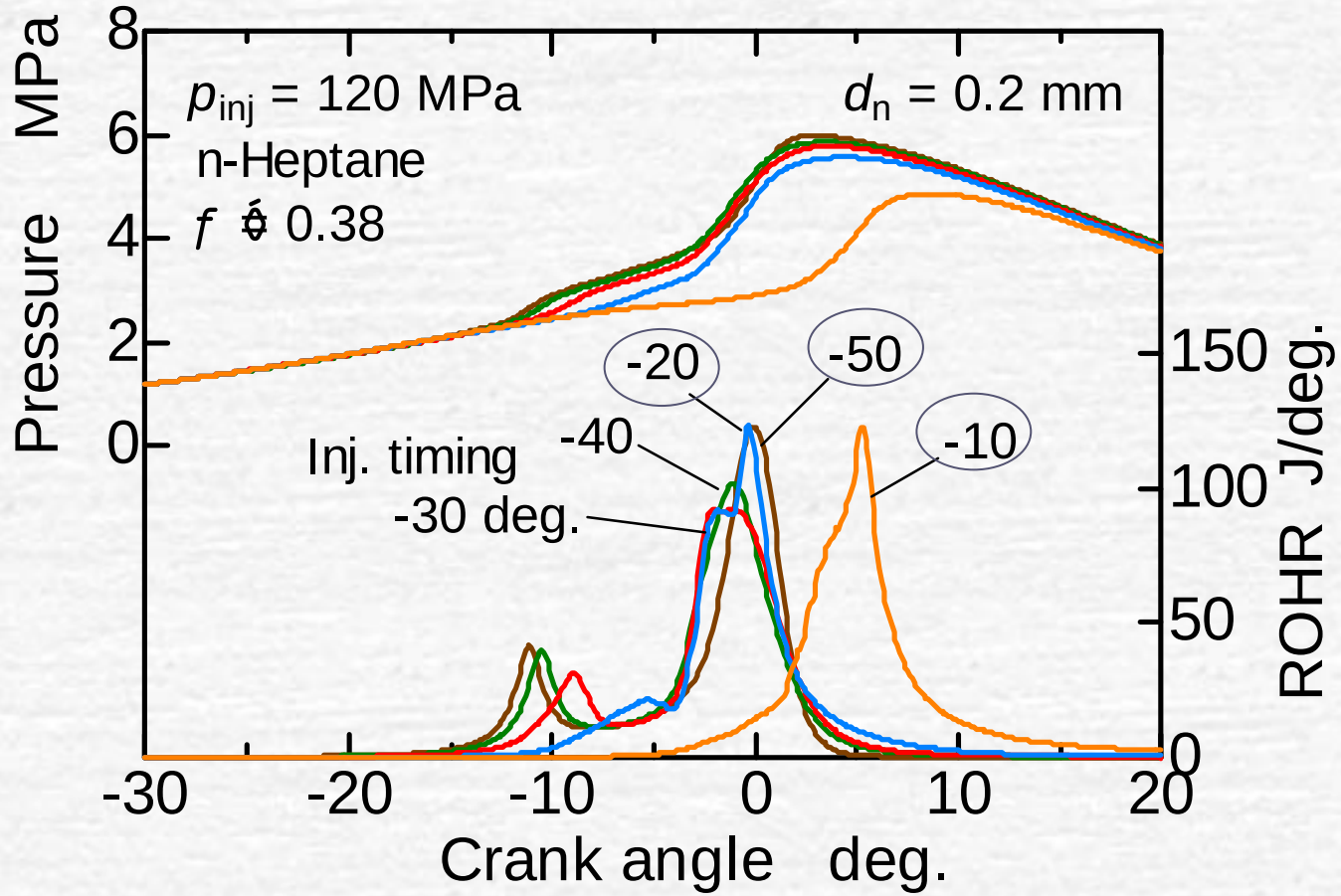

ϕ – T Map and NO Formation as Affected by Injection Timing

p_{inj} = 120 MPa, d_n = 0.2 mm × 4 holes

φ-T map at the time of maximum ROHR

Inj. Timing = -50 deg.

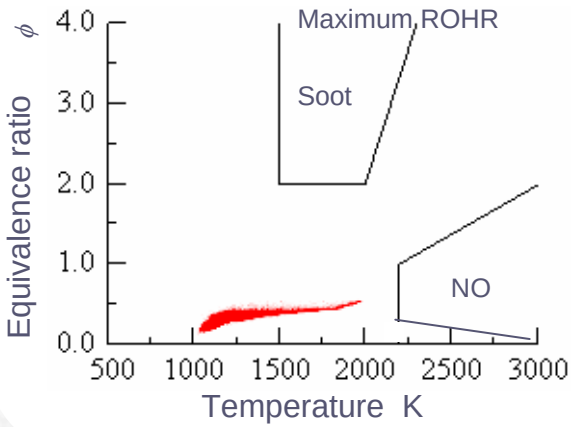

Inj. Timing = -30 deg.

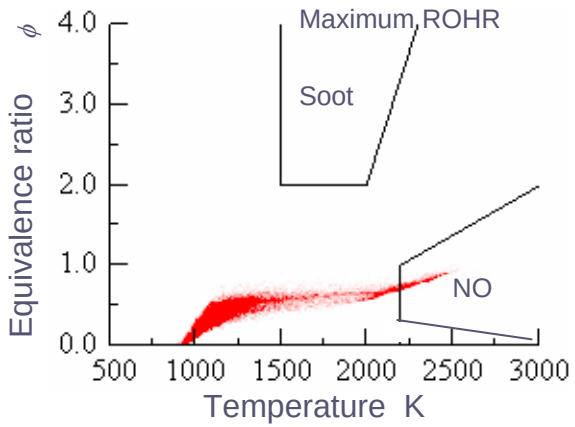

Inj. Timing = -10 deg.

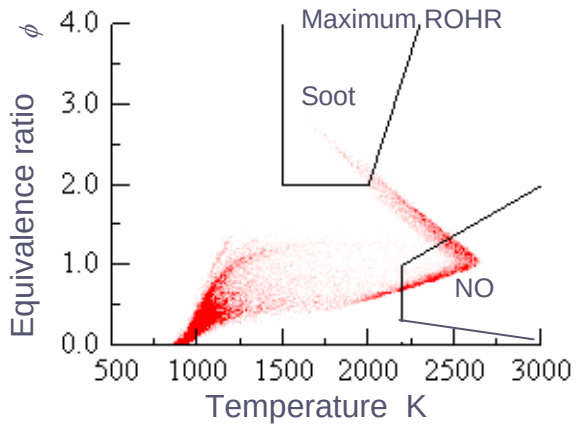

NO Formation and $dp/d\theta$ as affected by Injection Timing

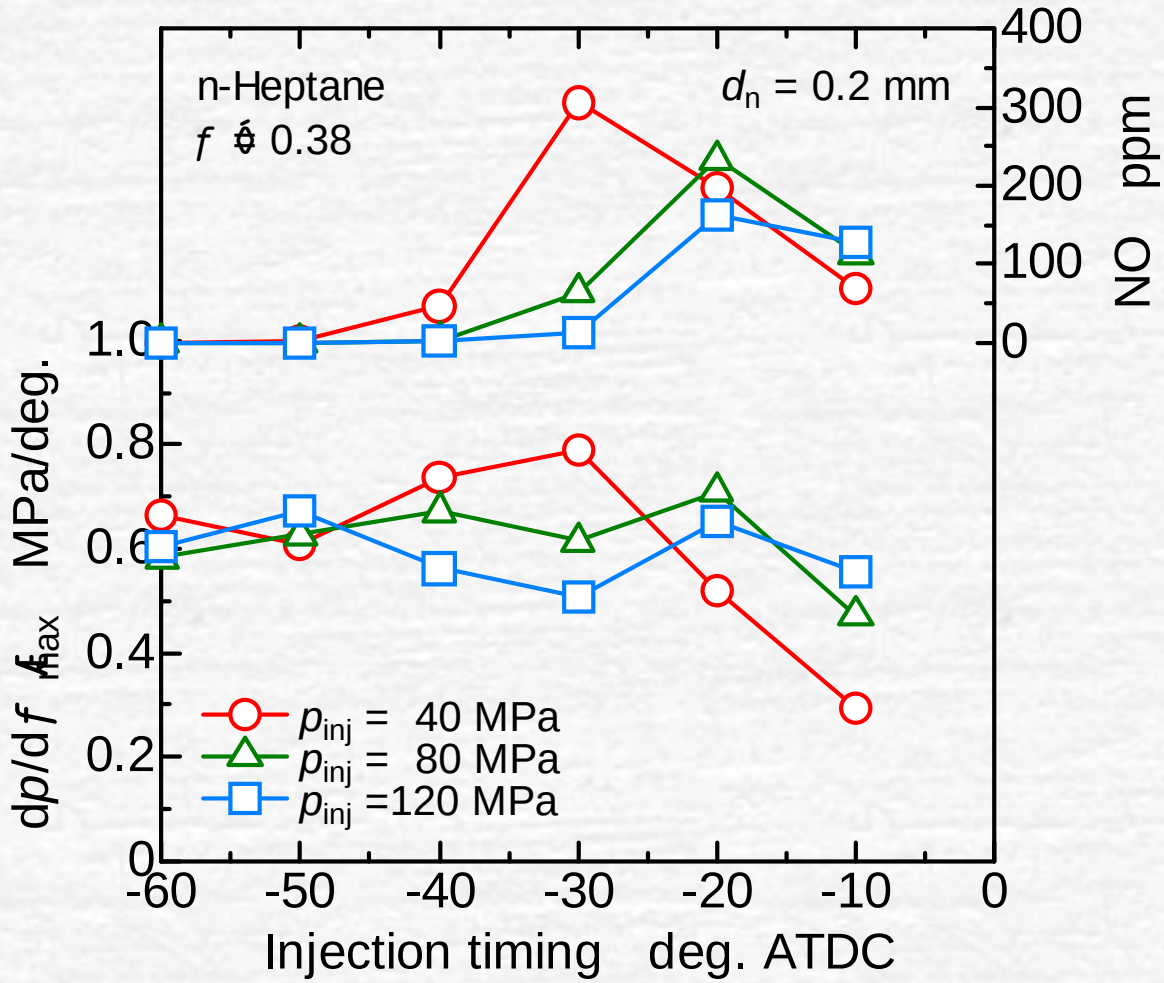

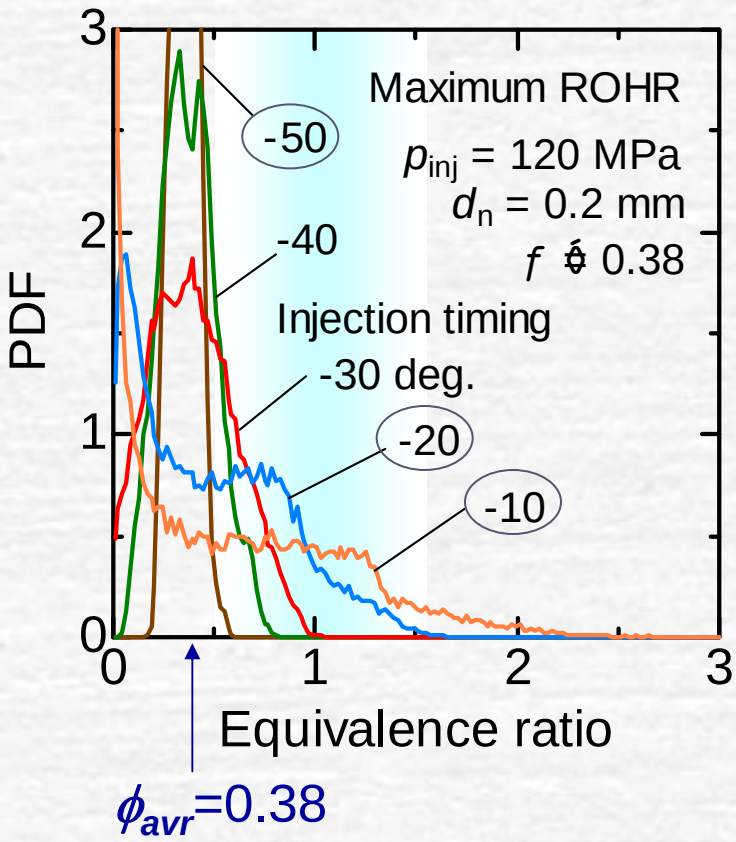

Comparison between LES and RANS – Local Heat Release Rate

p_{inj} = 120 MPa, d_n = 0.2 mm × 4 holes
Injection timing = 30 deg. BTDC

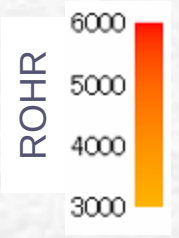

ROHR 3000 kJ/(m3 deg.) and over

LES

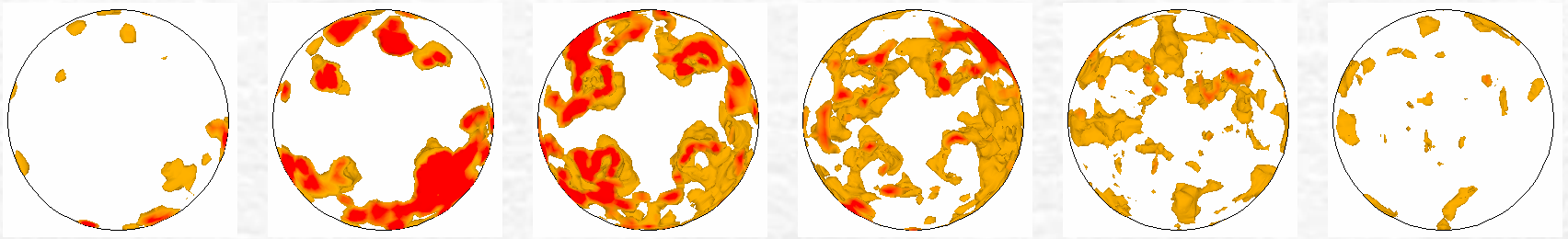

-3 deg. -2 deg. -1 deg. 0 deg. 1 deg. 2 deg.

RANS

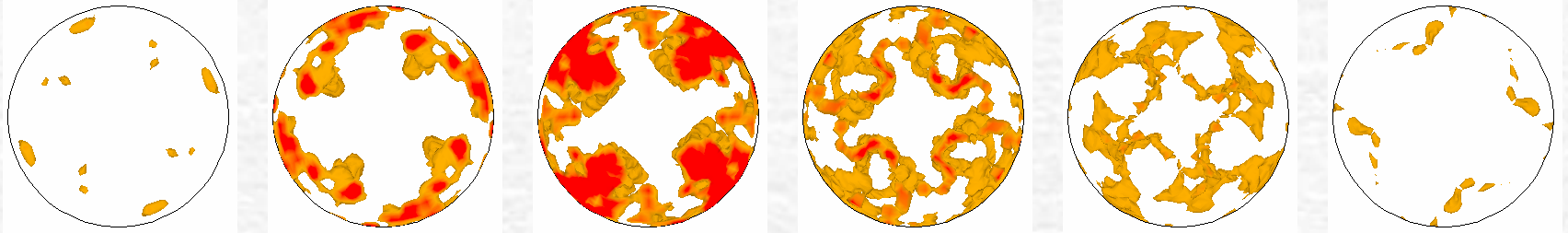

-3 deg. -2 deg. -1 deg. 0 deg. 1 deg. 2 deg.

Comparison between LES and RANS – Overall Heat Release Rate

p_{inj} = 120 MPa, d_n = 0.2 mm × 4 holes
Injection timing = 30 deg. BTDC

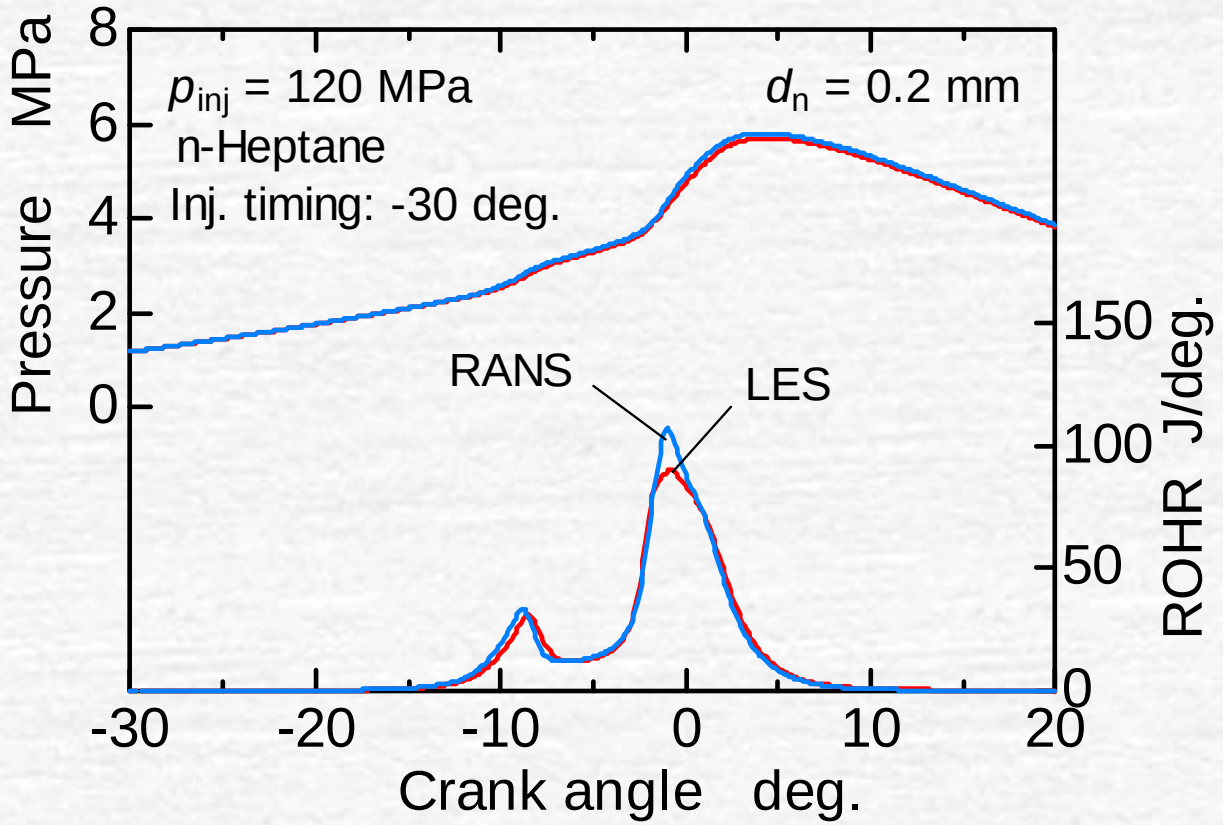

Conclusions

- The mixture formation and combustion have been analyzed by LES for Diesel/PCCI combustion under a partial load conditions, varying the fuel injection pressure and timing over a wide range.
- From the view point of NO production and pressure rise rate, optimum mixtures are the ones that are distributed in a wide range of equivalence ratios and at the same time.stay in a lean region.
- Such mixture distributions can be achieved by adjusting the injection timing. Higher injection pressures give better results.
- LES and RANS give nearly the same results for pressure and the overall heat release rate, whereas LES provides more realistic information of the local heat release rate.

END

Proceedings of the Thirtieth IEA/TLM, September, 14-18, 2008,Capri,Italy

LES Analysis for Controlling Fuel Distribution in Diesel PCCI Combustion

Subtask 3.1D

Kazuie Nishiwaki, Ritsumeikan University
nswk@fc.ritsumei.ac.jp
and
Takafumi Kojima
Takamatsu National College of Technology

ABSTRACT

The mixture formation and combustion have been analysed by LES for Diesel/PCCI combustion under a partial load conditions from the view point of NO emission and pressure rise rate. For the systematic analysis, varying the fuel injection pressure and timing over a wide range, effective sub-models have been integrated in the LES code: a gas jet model for fuel spray and Schreiber model, which comprises five step global model, for the low temperature oxidation and hot flame reaction along with the extended Zel'dovich model for NO formation. The gas jet model is shown to give reasonable results in predicting the penetration length of spray. Analyses of the computed results show that the optimum mixtures are the ones that are distributed over a wide range of equivalence ratios and at the same time stay in a lean region. Such mixture distributions can be achieved by applying a high injection pressure and by adjusting the injection timing.

INTRODUCTION

The diesel emissions regulation, which is going to be even more stringent in a near future, demands further improvement in emissions reduction of combustion itself as well as in catalytic converter performance. Though recent improvements in performance of catalytic converters are significant, one problem that is posed with the driving-mode test is that under low load conditions, especially when the cold start mode is included, the exhaust gas temperature is sometimes too low (less than around 200 °C) for a catalytic converter to be active. In such circumstances switching the combustion mode from Diesel at high loads to PCCI at low loads has a potential to improve the emissions performance. Because the PCCI features quite low NOx and PM emissions with a high thermal efficiency, though its output is restricted to a partial load.

The purpose of the study is to develop an efficient LES computer model for a systematic analysis of the mixture formation in the PCCI combustion mode from the view point of NO emission and pressure rise rate, varying the injection pressure and timing over a wide range.

OUTLINE OF THE MODEL

CFD Model The CFD model solves the transport equations for mass, momentum, enthalpy and species mass fractions in spatially filtered forms (LES). Sub-grid kinematic viscosity is expressed by Smagorinsky model, the model constant of which is assumed 0.1.

The engine used for the present calculations has a disk-shaped combustion chamber as shown in Figure 1. The cylinder bore and stroke are 82.3 mm and 114.3 mm, respectively, the compression ratio is set to 12.0. The number of numerical cells is 38,400, which gives [cell volume]$^{1/3}$=3.0 mm at bdc and 1.5 mm at tdc. These average cell sizes are less than the measured integral length scales, which are 4-5 mm at bdc and 2.5 mm at tdc for an engine similar in size, referring to the literature.

The engine speed is set to 1800 rpm. The wall temperatures are assumed to be 400 K and uniform over all the walls. The initial condition is given at the intake valve closing time or 146° btdc. The initial cylinder pressure is set to 0.1 MPa and the temperatures are assumed 323 K and uniform.

The initial instantaneous velocity field for the LES is given by the Method of Generating Correlation[1, 2], which was developed in Ritsumeikan University. This method is schematically shown in Figure 2 and briefly

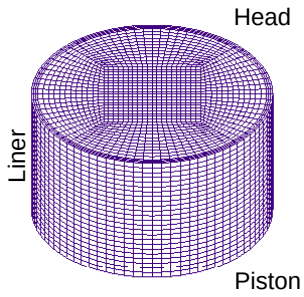

Figure 1 Computational cells

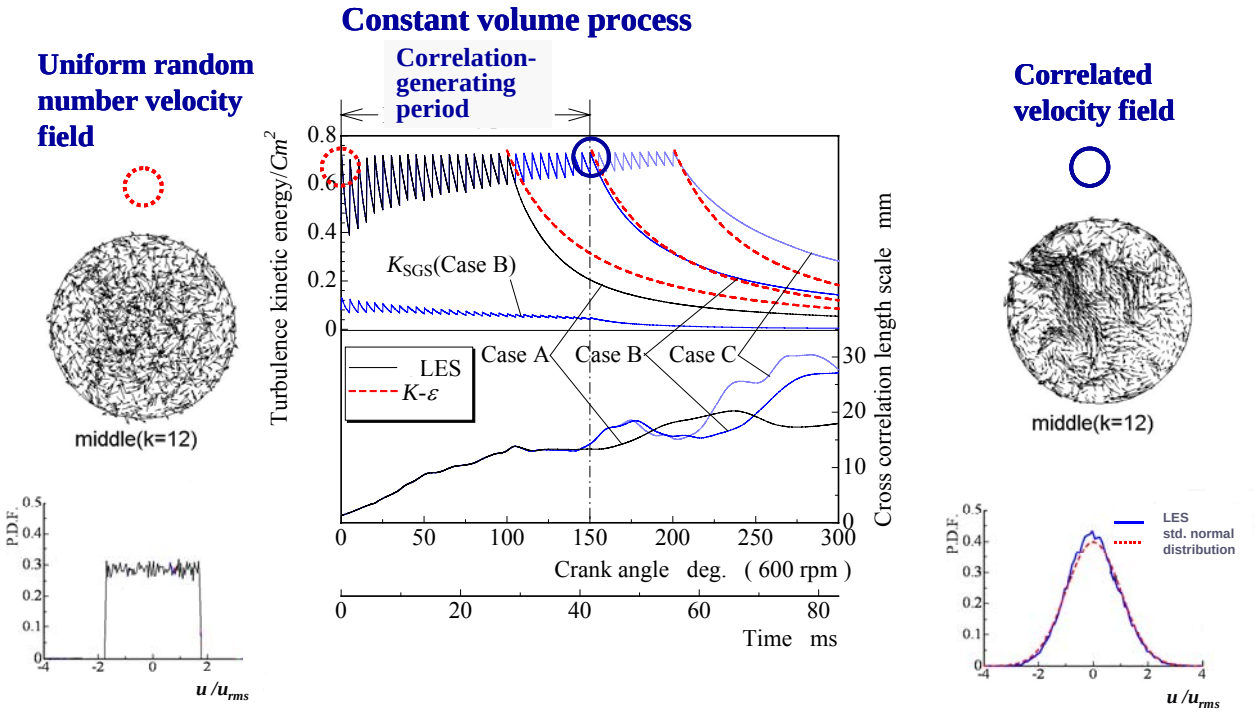

Figure 2 Method for generating initial instantaneous velocity field for LES

described as follows.

The first step is to give fluctuation velocities using uniform random numbers in a cylinder volume at the beginning of compression (intake valve closing time) for a pre-determined turbulence kinetic energy; the present calculation assumes [the turbulence kinetic energy]/C_m^2=0.74 (C_m: mean piston speed), which is a typical value for conventional engines. An example of the velocity field is shown on the left hand side of the figure. At this instance, the pdf of fluctuation velocities is rectangular in shape as shown in the figure. The second step is to begin the LES to compute the flow field, while the piston stops at the intake valve closing time keeping the cylinder volume constant. The turbulence kinetic energy decays due to the interaction between the fluctuation velocities. The third step is to pose the computation after an arbitral elapsed time (for example, several milliseconds) and to multiply every velocity fluctuation by the same constant value so as to return the turbulence energy to the initial value as a volume average. Then the LES restarts and repeats the same process until the turbulence kinetic energy dissipation reaches almost the same that is computed separately by the RANS for the same initial turbulence kinetic energy and the integral length scale, which is given referring to existing experimental results. The turbulence kinetic energy and the cross-correlation length scale during the repetitive process are shown in the figure. The cross-correlation length scale is zero at first and then increases, in other words, the correlations are generated between the fluctuating velocities. The final repetition is designated as Case B in the figure. The initial velocity field thus obtained is shown on the right hand side. The pdf of the fluctuation of velocities exhibits almost the standard normal distribution, which is the future of turbulent flows.

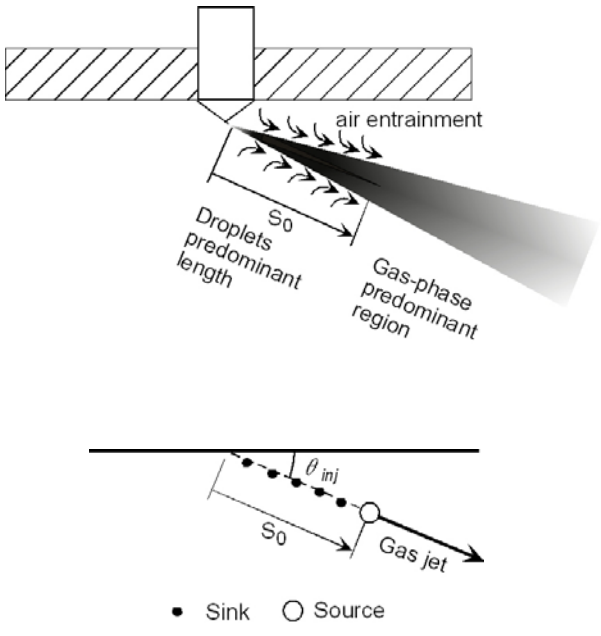

Figure 3 Gas jet model

Sub-models to be integrated in the CFD are a spray model and a reaction model. These models should be simple to make the computation effective for a systematic analysis changing the injection timing and the injection pressure in a wide range. They are described in the following.

Spray Model The gas jet model that was developed by Ikegami et al.[3] is adopted. As illustrated at the top of Figure 3, a spray is divided into two regions in the direction of injection. In the first region, the length of which is S_0, droplets are predominant, or densely populated, and the width of the region is so small that the

Table 1 Injection conditions studied

Nozzle hole diameter d_n	: 0.1, 0.2 mm
Injection angle θ_{inj}	: 30 deg.
Droplets predominant length S_0	: 20 mm
Injection pressure p_{inj}	: 40, 80, 120 MPa
Injection timing	: 10, 20, 30, 40 50, 60° btdc

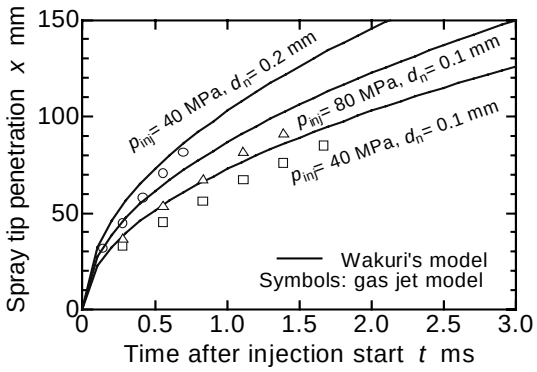

Figure 4 Comparison of spray tip penetrations computed by gas jet model and estimated by Wakuri's model

numerical cells are not enough in size to resolve droplets behaviours and mixing with entrained air. The second one is a gas-phase predominant region. The bottom part of the figure shows the gas jet model. It assumes the first region as several sinks placed in cells that model the air entrainment. The mass of air entrained is estimated by Wakuri's model[4]. The source, placed at the end of a series of the sinks, ejects the mixture of evaporated fuel and air with the sum of momentum of the fuel injected and the air entrained through the sinks. No velocity fluctuations are given at the source as a boundary condition, since the length scale at the nozzle is so small that the cell size can't resolve and in addition such small turbulence components may be dissipated quickly. Major turbulence induced by the jet is computed by the LES itself as the interaction with surrounding gas that fluctuates.

The injection conditions that were studied are shown in Table 1. The number of different combinations of nozzle diameter, injection pressure and injection timing is 2x3x6=36. The computing time was 15-20 hours each combination.

Figure 4 shows the penetration length x computed by the gas jet model and that estimated by Wakuri's model, which is shown below:

$$x = \left(\frac{2c(p_{inj} - p_a)}{\rho_a} \right) \left(\frac{t\, d_n}{\tan\theta} \right)^{0.5} \qquad (1)$$

where, p_a: ambient pressure, t: time, θ: spray angle, c: empirical constant. The spray angle θ is given by an empirical relation.

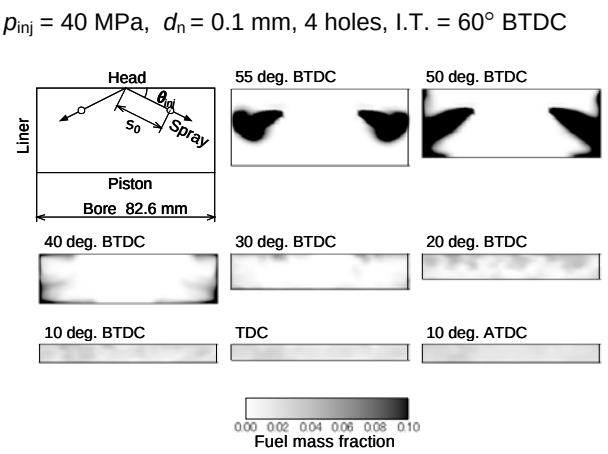

Figure 5 Mixture formation computed by gas-jet model

It is seen in the figure that the gas jet model compares well to Wakuri's model.

Reaction Kinetics The reaction kinetics for hydrocarbon fuel to be combined with the transport equations is given by the five step global model, proposed by Schreiber et al[5]. The model includes both the low temperature oxidation and hot flame reaction. Normal-heptane was used as fuel. Using the zero-dimensional model, the frequency factors and the activation energies of the reaction kinetics were adjusted to give the best fit to the measurements presented by Tsurushima et al. [6]. Thermal NO formation is modeled by the extended Zel'dovich mechanism.

The average equivalence ratio and EGR ratio were set to 0.38 and 0.07, respectively.

GENERAL PERSPECTIVE ON MIXTURE FORMATION AND PCCI COMBUSTION

Figure 5 illustrates an example of the mixture formation computed by the gas jet model for no-reaction case. The injection timing is as early as 60° btdc in this case. Nevertheless the fuel mass fraction near TDC still shows heterogeneous distribution in some degree. The degree of heterogeneity in mixture at the time of ignition is controlled by the injection timing, nozzle diameter and injection pressure, which will be discussed in a later section.

Figure 6 illustrates combustion cases, showing local heat release rates, for three different injection timings under the condition of injection pressure p_{inj}=120MPa and nozzle hole diameter d_n=0.2 mm. To see the details of the differences in the local heat release rate, the values of 3000 kJ/(m^{3}deg.) and over are shown. It is seen that as the injection timing advances differences between the local heat release rates becomes smaller and at the same time the combustion duration becomes shorter. This tendency corresponds to the difference in the equivalence ratio distribution between the three different injection timings during combustion, which will be shown next.

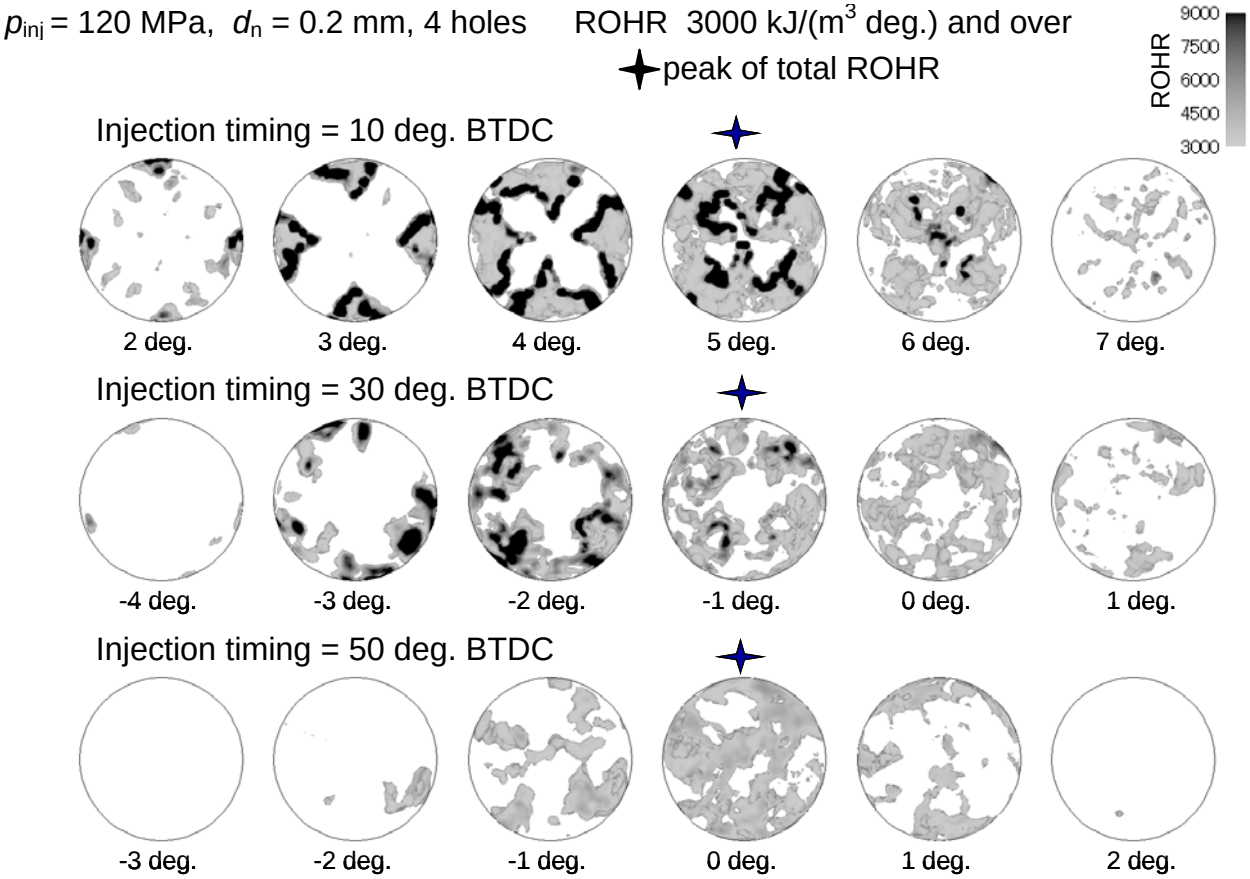

Figure 6 Local rates of heat release for three different injection timings

ANALYSIS OF HEAT RELEASE RATE AFFECTED BY MIXTURE FORMATION

Figure 7 shows the rms of fuel mass fraction fluctuations as a function of crank angle for two different injection pressures and three different injection timings. In every case, the rms values jumps up upon the start of injection to increase until the end of injection and then decays as the spray mixes with surrounding air. The tendencies are seen to be the same for all cases. The only difference is that the rms value increases and decays faster for injection pressure p_{inj}=120 MPa than for p_{inj}=40 MPa.

The above-mentioned difference is reflected in the time change in the pdf of local equivalence ratio as shown in Figure 8. The pdf is distributed in a narrow range for the injection pressure p_{inj} =120 MPa compared to that for p_{inj} =40 MPa under each injection timing condition.

The difference in combustion appearance between the three injection timings shown in Figure 6 corresponds to the difference in the pdf of local equivalence ratio as described in the following. As can be seen, for injection timing θ_{inj}=-10° atdc and injection pressure p_{inj} =120 MPa, considerable amounts of mixtures are distributed near stoichiometric equivalence ratio. The fact explains that comparatively strong local heat release rates appear for that injection timing in Figure 6. On the other hand, for θ_{inj}=-50° atdc most mixtures are seen near the equivalence ratio(=0.38), resulting in lower local heat

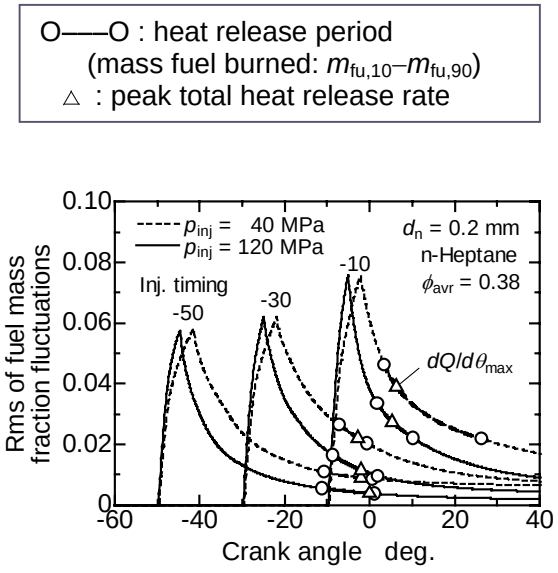

Figure 7 RMS of fuel mass fraction fluctuations as function of crank angle for two different injection pressures and three different injection timings

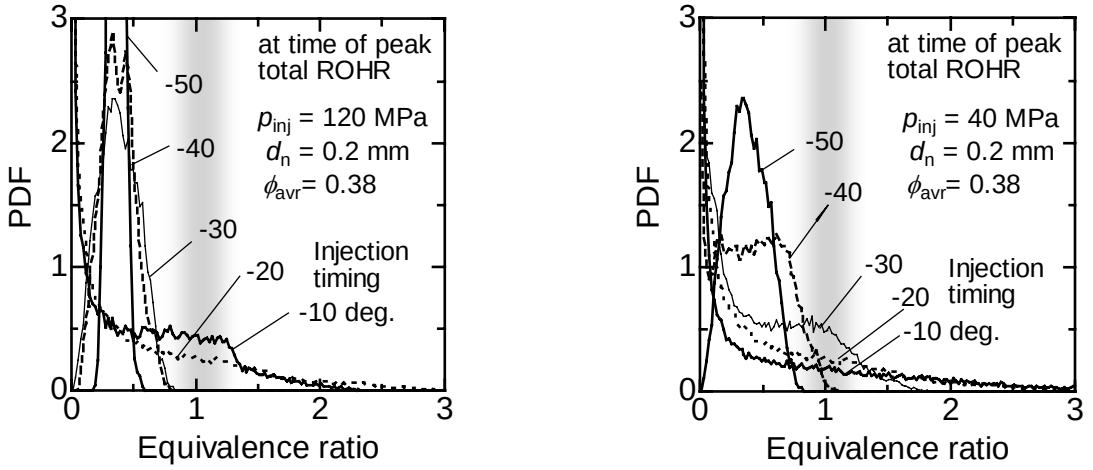

(a) injection pressure p_{inj} =120 MPa (b) injection pressure p_{inj} =40 MPa

Figure 8 PDF of local equivalence ratio at time of peak total rate of heat release for (a) injection pressure p_{inj} =120 MPa and (b) p_{inj} =40 MPa

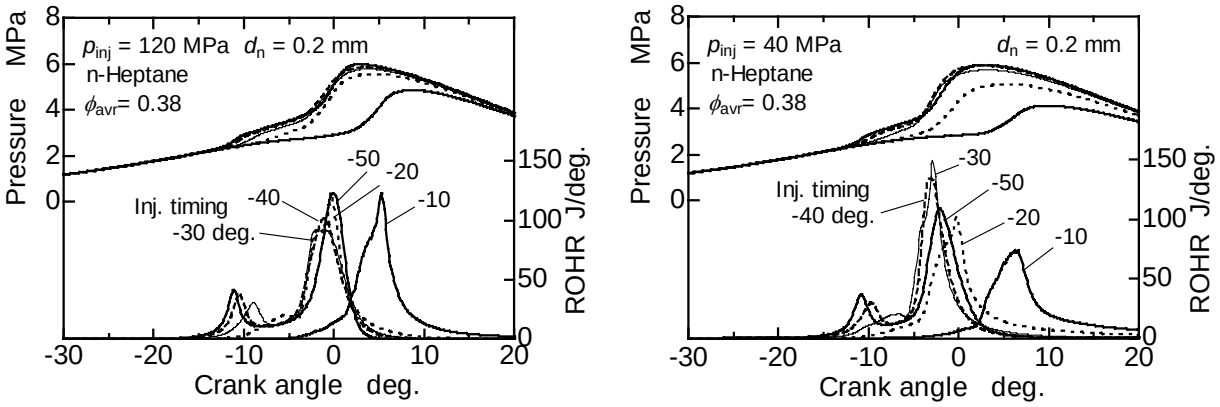

(a) injection pressure p_{inj} =120 MPa (b) injection pressure p_{inj} =40 MPa

Figure 9 Pressures and total heat release rates as function of crank angle for (a) injection pressure p_{inj} =120 MPa and (b) p_{inj} =40 MPa

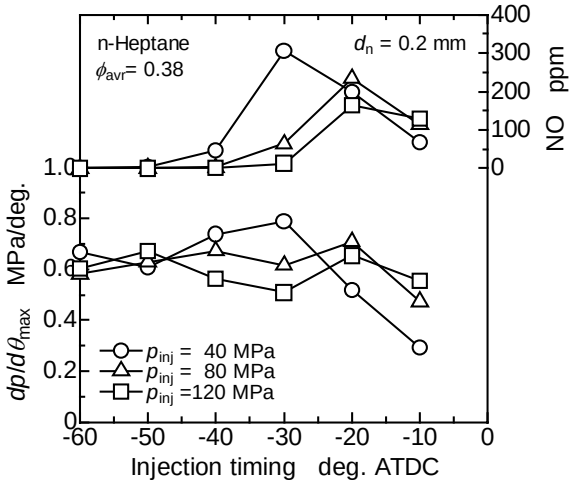

Figure 10 Maximum values of $dp/d\theta$ and NO formation as function of injection timing

release rates spreading in a wide area in the combustion chamber. For θ_{inj}=-30° atdc, all the mixtures stay in the lean side and are distributed in a wide range, exhibiting the intermediate tendency of the local heat release rates in Figure 6.

Figure 9 shows pressures and the total heat release rates for the two injection pressure conditions. In both the conditions, the total heat release rates for all injection timings except -10° atdc exhibit the feature of the PCCI combustion, in which the low temperature oxidation appears first and then the hot flame reaction follows. For θ_{inj}=-10° atdc, the time difference between the low temperature oxidation and the hot flame reaction becomes so short that the two reactions are difficult to separate in appearance.

In Figure 9(a) (p_{inj} =120 MPa), the peak values are seen to be higher for θ_{inj}=-10° atdc and -20° atdc. This is due to that considerable amounts of mixtures are in the nearly stoichiometric range as can be seen in Figure 8(a). This is also the case for θ_{inj}=-30° atdc in Figure 9(b) (p_{inj} =40 MPa). Another case of higher peak value in Figure

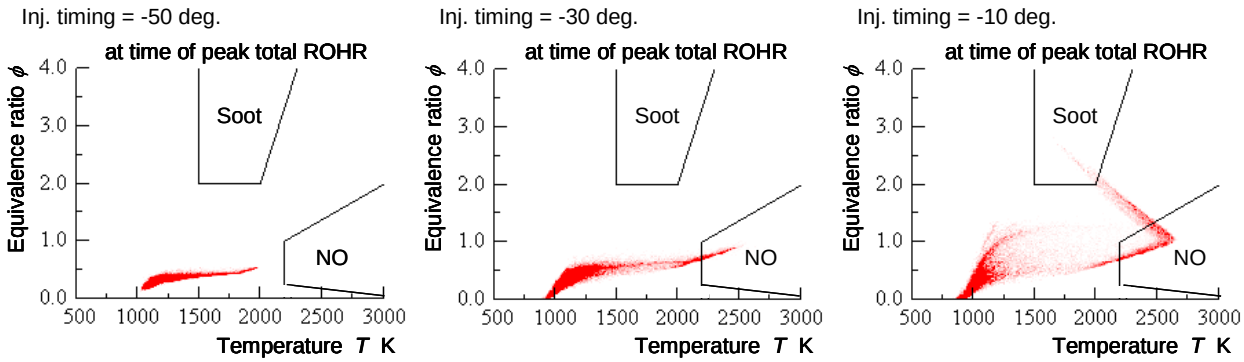

(a) Injection pressure p_{inj} =120 MPa, nozzle hole diameter d_n=0.2 mm

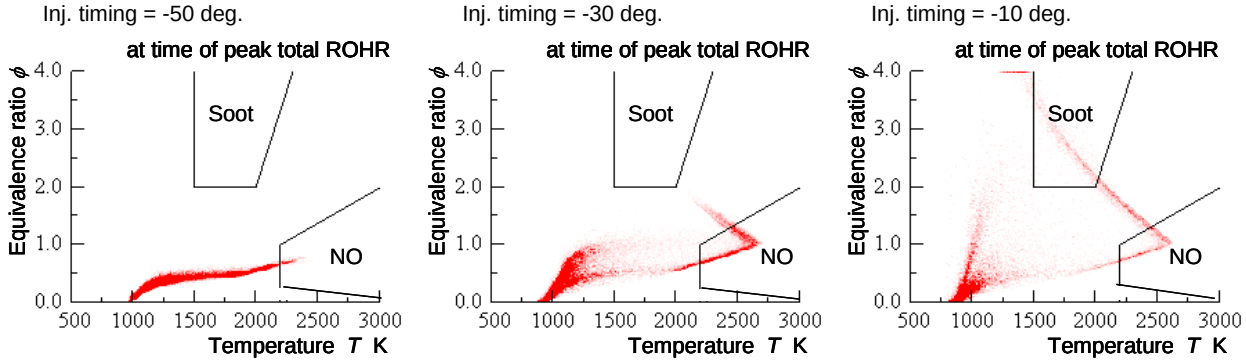

(b) Injection pressure p_{inj} = 40 MPa, nozzle hole diameter d_n=0.2 mm

Figure 11 ϕ–T maps for injection timings θ_{inj}=-50, -30 and -10° atdc and for injection pressures p_{inj} = 120 and 40 MPa

9(a) is seen for θ_{inj}=-50° atdc. In this condition, the mixture is almost homogeneous with the value of the average equivalence ratio (=0.38) as seen in Figure 8(a) and therefore the local reactions take place nearly at the same time in a large part of the combustion chamber volume, producing the high peak of total heat release rate.

Referring to the lower peaks of total heat release rate in Figure 9(a) that are seen for θ_{inj}=-30° atdc and -40 ° atdc, the pdf of the mixtures are distributed as wide as over the range between 0 and stichiometric values. Such mixtures have locally different ignition times and reaction speeds from each other, making the overall reaction slower and hence peak pressure lower. This is also the case for θ_{inj}=-50° atdc in Figure 9(b).

As the summary of the above discussions the maximum values of $dp/d\theta$ are shown as a function of injection timing in Figure 10. In general an acceptable value of the maximum values of $dp/d\theta$ for conventional diesel engines is less than around 0.5 MPa/deg. From this stand point, The allowable values of $dp/d\theta$ are seen at θ_{inj}=-30° atdc for p_{inj} =120 MPa, at θ_{inj}=-10° atdc for p_{inj} =80 MPa and at θ_{inj}=-20° atdc and at θ_{inj}=-20° atdc for p_{inj} =40 MPa.

NO FORMATION

Figure 11 shows ϕ–T maps (ϕ : local equivalence ratio, T: local temperature) at the time of peak total rate of heat release for θ_{inj}= -50, -30 and -10° atdc and for p_{inj} = 120 and 40 MPa. It is seen that for θ_{inj}=-10° atdc and p_{inj} =120 MPa, the mixtures are distributed in a wide range of equivalence ratio from lean to rich conditions to cover both the regions of NO and soot formation, whereas for θ_{inj}=-50° atdc most mixtures are distributed in the range of ϕ less than 0.5 covering neither NO nor soot formation region. For p_{inj}=40 MPa, the tendency is the same in a more pronounced way. Thus, as the injection timing is advanced the amount of near-stoichiometric and rich mixtures decreases to produce less NO and less soot.

The NO formation at the end of combustion are shown as a function of injection timing for p_{inj}=120, 80 and 40 MPa in the upper part of Figure 10. It can be said that the higher injection pressures and the earlier injection timings are favorable from the emission stand point. From both the stand points of NO emission and the maximum value of $dp/d\theta$, the combination of p_{inj}=120 MPa and θ_{inj}=-30° atdc gives the best result within the conditions tested.

CONCLUSIONS

The mixture formation and combustion have been analyzed by LES for Diesel/PCCI combustion under a partial load conditions. For a systematic analysis varying the fuel injection pressure and timing over a wide range, efficient sub-models have been employed; the gas-jet model for fuel spray, Schreiber model, which is made up

of five global reactions, for combustion, and the extended Zel'dovich model for NO formation. It is shown that the gas-jet model gives a reasonable result in predicting the spray penetration.

From the view point of NO formation and pressure rise rate, optimum mixtures are the ones that are distributed in a wide range of equivalence ratios and at the same time stay in a lean region.

Such mixture distributions can be achieved by applying a high injection pressure and by adjusting the injection timing.

ACKNOWLEDGEMENT

This study is partially supported by JSME Technical Committees RC-232 and RC-226.

REFERENCES

[1] Saijyo, K., Nishiwaki, K. and Yoshihara, Y., "A Numerical Prediction Method for the Auto-Ignition Process in a Homogeneous Charge Compression Ignition Engine," SAE Spring Fuel & Lubricants Meeting, Paper No. 2003-01-1818, 2003.

[2] Nishiwaki, K. and Saijyo, K., "A Numerical Analysis of the Premixed Charge Compression Ignition Combustion by LES", Proc. the twenty-sixth IEA/TLM, August, 2004, Helsinki.

[3] Ikegami, M. et al., Trans. JSME, Ser. B, Vol. 53, No. 491, 1987, pp. 2241-2250.

[4] Wakuri, Y. et al., Trans. JSME, Vol. 25, No. 156, 1959, pp. 820-826.

[5] Schreiber, M., Sakak, A. S. Lingens, A. and Griffiths, J. F., "A Reduced Thermokinetic Model for the Autoignition of Fuels with Variable Octane Ratings," 25th Symp. (Int.) on Comb., 1994, pp. 933-940.

[6] Tsurushima, S. et al., Proc. the 17th Internal Combustion Symposium, No. 61, 2002, pp. 339-344.